Catal Lett (2009) 129:344–349
DOI 10.1007/s10562-009-9863-8

Photooxidation Products of Ethanol During Photoelectrochemical Operation Using a Nanocrystalline Titania Anode and a Two Compartment Chemically Biased Cell

Maria Antoniadou · Dimitris I. Kondarides · Panagiotis Lianos

Received: 20 October 2008 / Accepted: 7 January 2009 / Published online: 4 February 2009

Abstract Production of hydrogen and/or electricity by photocatalytic treatment of aqueous ethanol solutions has been investigated in a two compartment chemically biased photoelectrochemical cell, employing commercial nanocrystalline Titania as photoanode and Pt as cathode. Results show that hydrogen is produced during photooxidation of ethanol by cathode reduction and by means of a flow of external electric current. The performance of the cell decreased after several hours of operation, most possibly due to the formation of hydrocarbons of higher molecular weight. This is contrary to simple photocatalytic ethanol oxidation where complete mineralization of alcohol is observed.

Keywords Titanium dioxide · Ethanol photooxidation · Photoelectrochemical cell · Photooxidation intermediates · Hydrogen production

1 Introduction

Photocatalytic decomposition of aqueous solutions of organic substances under anaerobic conditions can lead to production of hydrogen. The process can be simply described as follows: a semiconductor photocatalyst is excited by absorption of photons generating electron–hole pairs. Holes oxidize organic substrates liberating hydrogen ions, among other oxidation products. Hydrogen ions are in turn reduced by excited electrons, producing hydrogen molecules. This simple and straight forward process has to compete with electron–hole recombination. To suppress recombination, several techniques have been devised, most popular among them being the so-called photocatalytic (PC) process [1–13] and the photoelectrochemical (PEC) process [14–16]. In the PC case, noble metal nanoparticles are deposited on the nanostructured semiconductor. The metal nanoparticles act as electron traps, which impede recombination and facilitate transfer of electrons to reduce hydrogen ions, thereby decreasing the overpotential for H_2 evolution. In the PEC case, the nanocrystalline semiconductor is deposited on an electrode, which acts as the anode. The cathode is made of a high work function metal; typically Pt. Excited electrons are channeled through an external circuit to the cathode. Hydrogen ions are then reduced at the cathode producing molecular hydrogen. In the present work, photocatalytic oxidation of ethanol has been studied by employing the PEC operation.

Both PC and PEC process lead to the same result, that is, oxidation of the target substance and production of hydrogen. PC process is more efficient, since it operates at the nanoscale, where one semiconductor nanoparticles with a deposited metal nanoparticle operates as a nanoreactor. The PEC process, however, has other advantages, the most notable being the fact that production of hydrogen is accompanied by electric current flow. If the anode and cathode are placed in two separate compartments communicating with a proton-transfer membrane (for example, Nafion), it is possible to run the cathode compartment under aerobic conditions, where hydrogen generates water and the cell then operates as a photo-fuel cell [14]. The photo-fuel cell can be used to produce electricity by consuming surplus waste materials or water pollutants [14].

M. Antoniadou · P. Lianos (✉)
Engineering Science Department, University of Patras,
26500 Patras, Greece
e-mail: lianos@upatras.gr

D. I. Kondarides
Department of Chemical Engineering,
University of Patras, 26500 Patras, Greece

Such a cell is also studied in the present work, employing ethanol as model target substrate.

Production of hydrogen by photocatalytic treatment of aqueous solutions of ethanol (EtOH) is being studied for several decades [1–13]. A revived interest has been recently demonstrated [8–13, 17] owing to the pressing need for renewable energy resources. It has thus been shown that photocatalytic treatment of EtOH under unaerated conditions proceeds in steps that can be summarized by the following photoreforming reaction [9–11]:

$$C_2H_5OH + 3H_2O \rightarrow 2CO_2 + 6H_2. \qquad (1)$$

According to Reaction (1), ethanol is completely mineralized in the presence of water, producing CO_2 and H_2. Thus, photoreforming is realized by oxidation of the substrate towards compounds of progressively lower molecular weight, as it will be discussed later. However, during PEC operation, we realized that this might not be exactly the case, when the photoelectrochemical route is actually chosen. We have then decided to analyze the oxidation products during a PEC oxidation of ethanol to make the situation more clear. Subsequently, the present work focuses attention on the progress of EtOH oxidation in a two compartment PEC cell.

2 Experimental

2.1 Materials

The nanocrystalline Titania used in the present work was commercial Degussa P25, which consists of 25–30 nm nanoparticles. All other reagents were obtained from Aldrich and Merck, while Millipore water was used in all experiments. SnO_2:F transparent electrodes (resistance 8 Ω/square) were purchased from Hartford, USA.

2.2 Preparation of Nanocrystalline Titania Films and Anode Electrodes

Nanocrystalline Degussa P25 was dispersed in aqueous Carbowax solution [18], as previously described [15]. Carbowax solution was prepared according to the following recipe: 8.5 mL of water were mixed with 10.5 mL of EtOH. To this mixture we added 0.8 mL of a concentrated polyethylene glycol (PEG) 2000 aqueous solution made of 30 g PEG 2000 and 30 g water. Degussa P25 was dispersed in this aqueous Carbowax solution by mixing 0.3 g Degussa with 3 mL of the solution. The resulting material was a white paste, which can be easily cast on any solid substrate. Films were thus made by casting the paste on SnO_2:F transparent electrodes. After casting, the films were calcined at 550 °C. This relatively high temperature was necessary to assure that all organic templates were destroyed and removed from the photocatalyst surface. High calcination temperature adversely affects the conductivity of the transparent conductive electrode. This problem is less pronounced when SnO_2:F is used, as in the present case (compared, for example, to indium–tin-oxide, ITO, electrodes). The procedure was repeated once more in order to increase the amount of deposited photocatalyst. The final quantity of Titania on the support was 25 mg, while the geometrical dimension of the film was $4 \times 2.5 = 10$ cm^2. Thanks to the high calcination temperature, the film adhered well on the support and withstood the hard alkaline conditions applied during PEC operation. A photograph of a film thus prepared is shown in Fig. 1a, depicting also the wire connection, which was made by means of a copper ribbon attached on the uncovered part of the SnO_2:F electrode.

2.3 Description of the Reactor

The PEC cell was a two compartment (H-shaped) reactor made of Pyrex glass, schematically shown in Fig. 1b. The anode was made of one single SnO_2:F electrode with deposited nanocrystalline Titania, while the cathode was a Pt wire. The electrolyte of the anode compartment contained 1.0 mol L^{-1} NaOH and that of the cathode contained 1.0 mol L^{-1} H_2SO_4. These different electrolytes were used to apply a chemical forward bias between anode and cathode. The cathode compartment was either continuously

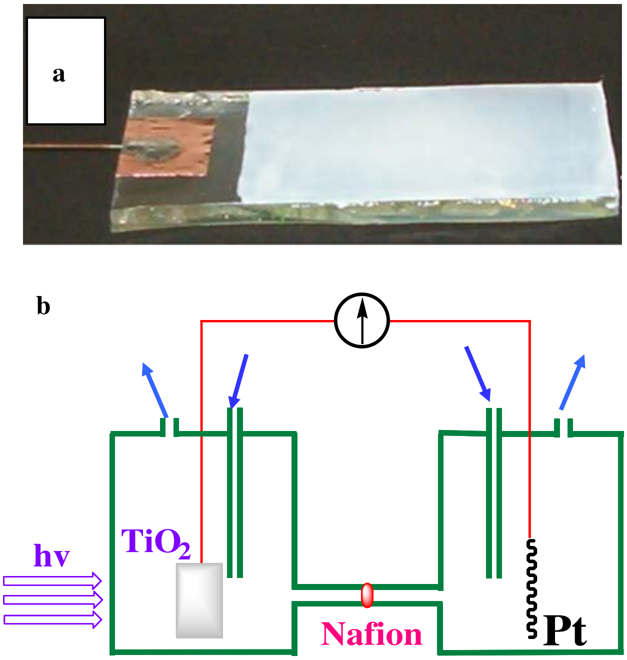

Fig. 1 **a** Photograph of the anode assembly depicting transparent conductive electrode, Titania film and wire connection; **b** schematic representation of the H-shaped PEC reactor

supplied with air by means of a small pump to run under aerobic conditions or with Ar gas to produce hydrogen under anaerobic conditions. In the latter case, Ar also served as a means of carrying product gases to a gas chromatograph for on-line analysis.

Exciting radiation was generated by a homemade lamp housing employing Black Light tubes with their spectral maximum located at around 360 nm [13]. Four tubes of 4 W nominal power each were symmetrically placed inside a cylindrical cavity with reflective wall. The intensity of incident radiation at the position of the film was measured with the use of a radiant power meter facing a single Black Light tube and was found to be 0.80 mW/cm^2. Since the photoanode can absorb light from all four tubes, we roughly estimate that the total light intensity incident on the photoanode was $4 \times 0.80 = 3.2$ mW/cm^2.

2.4 Measurements

UV–Vis absorption measurements were carried out with the use of a Cary 1E spectrophotometer. The intensity of radiation at the position of the catalyst was measured with a radiant power/energy meter (Oriel-70260). Electrical measurements were made with a Keithley 196 multimeter. Detection of product hydrogen was made online by using an SRI 8610C gas-chromatograph equipped with a molecular sieve 5A column and a TCD detector. The carrier gas was high purity Ar (99.999%). Samples were periodically collected via an automatic gas sampling valve and the concentration of H_2 present in the reactor effluent was determined as a function of time of irradiation. Calibration of the GC signal was accomplished with the use of a standard mixture of 0.25% H_2 in Ar. Reaction products in solution were identified with the use of a gas chromatography-mass spectrometry (GC/MS) system. The GC (Hewlett Packard 6890) was equipped with an HP-1MS capillary column (30 m × 0.25 mm × 1.0 μm film thickness) and was interfaced directly to the MS (HP 5973) used as detector [19]. Analysis was performed at a constant oven temperature of 40 °C. Identification of the GC/MS spectral features has been achieved with the use of a build-in library.

3 Results and Discussion

3.1 Photoelectrochemical Treatment of a Water–Ethanol Mixture

The above described PEC reactor was used to photocatalytically treat a 50%v. water–ethanol mixture. This mixture approximately corresponds to the molar ratio of ethanol/water involved in the photoreforming Reaction (1). As already said, the anode compartment also contained 1.0 mol L^{-1} NaOH and the cathode compartment 1.0 mol L^{-1} H_2SO_4. Alcohol was introduced in the anode compartment, in the presence of the nanocrystalline Titania electrode. The pH in the cathode compartment was 1.2 and in the anode compartment 13.6. The difference $\Delta pH = 12.4$ corresponds to a forward bias of 732 mV, according the rule: $\Delta V = 0.059 \cdot \Delta pH$ [16]. In a typical experiment, the photoanode was continuously illuminated for a period of 20 h.

Several separate experiments were run by setting the anode or the cathode compartment under aerobic or anaerobic conditions. When the cathode was run under anaerobic conditions, both electric current and hydrogen evolution was monitored during operation. When the cathode was run under aerobic condition, only the electric current was monitored. In contrast, results obtained under different cathode conditions were not detectably affected by the conditions under which the photoanode was run (aerobic or anaerobic).

Figure 2 shows the evolution of the short-circuit current and the hydrogen production rate recorded during anaerobic operation of the (dark) cathode. Data have been collected by passing an Ar stream through the cathode compartment and through the on-line gas chromatograph. The photoanode and the dark cathode were simply short-circuited through the current-measuring multimeter. First interesting finding extracted from Fig. 2 are that a substantial quantity of hydrogen was indeed produced by the above PEC operation. When the cell was run in the absence of EtOH or any other additive, both current and hydrogen evolution rate were one order of magnitude lower [15]. Once more, it is thus verified that the oxidation of the organic sacrificial agent present in the photoanode is mainly responsible for the cell performance [15]. Second interesting finding was that curves corresponding to short-

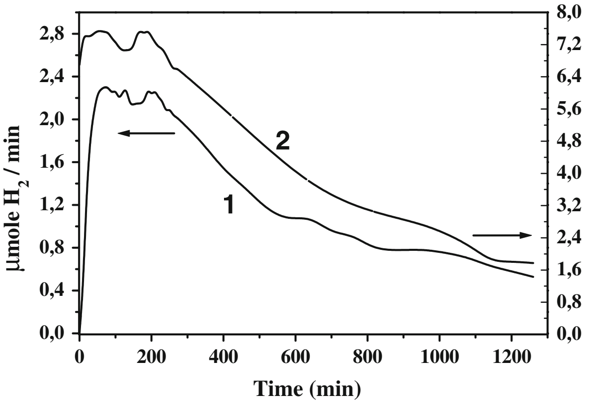

Fig. 2 Hydrogen production rate *1* and short-circuit current *2* in a two compartment PEC cell containing 1.0 mol L^{-1} NaOH + 50%v. EtOH in the anode compartment and 1.0 mol L^{-1} H_2SO_4 in the cathode compartment (run in an Ar flow)

circuit current and hydrogen production rate go in parallel, i.e., they exhibit a qualitatively similar dependence on irradiation time. This justifies the above assertion that molecular hydrogen is generated by reduction of hydrogen ions by electrons photogenerated at the photoanode and channeled through the external circuit to the dark cathode. Figure 2 also shows that both current and hydrogen evolution rates progressively decrease in the course of the 20 h that this experiment lasted. The reason for the observed deterioration of cell performance with time is not clear, and could be due to the effect of several parameters. One obvious reason is the progressive consumption of the acidic content of the cathode compartment. This has been confirmed by the fact that both current and hydrogen evolution rate increased when the electrolyte of the cathode compartment was renewed by a fresh solution. However, the initial conditions were not recovered. We believe that one main cause for the deterioration of the cell performance is the progressive evolution of the electrolyte content in the anode compartment. For this reason, the following analysis has been performed.

3.2 Identification of Reaction Intermediates in Solution

After several hours of UV treatment, the electrolyte in the anode compartment obtained a pale yellow color, which was obviously due to a species being formed during treatment. This species absorbed light in the UV–Vis spectral region, as can be seen in Fig. 3. In order to identify species present in the anode compartment, the obtained solution was then concentrated in a rotary evaporator and analyzed by means of GC/MS. Chromatograms obtained from this concentrated solution were characterized by an intense peak (at $t = 1.3$ min) due to unreacted ethanol (C_2H_5OH) and a peak of similar intensity (at $t = 1.1$ min) due to acetaldehyde (CH_3CHO). Two more peaks of substantially lower intensity (less than 10% of that of ethanol and acetaldehyde), located at $t = 1.5$ and 3.3 min, have been assigned with certainty to acetone (C_3H_6O) and 2-butenal (crotonaldehyde, C_4H_6O), respectively. Two additional chromatographic peaks could be observed at higher retention times, which correspond to compounds of higher molecular weight. However, these compounds could not be identified with certainty under the present experimental conditions. For this, a more detailed investigation is necessary, which is beyond the scope of the present study.

3.3 Proposed Reactant Pathway

Results of our recent studies obtained over irradiated aqueous Pt/TiO_2 suspensions [9–11] have shown that photocatalytic treatment of organic compounds in solution results in the progressive oxidation of the organic substrate by photogenerated holes (h^+) toward CO_2, which is accompanied by reduction of water by photogenerated electrons (e^-) and evolution of hydrogen. The overall reaction, termed as photoreforming, has been found to be nonselective with respect to the organic substrate employed and, therefore, practically all organic compounds in solution or in suspension may be used as feedstock for hydrogen production, including organic pollutants and biomass-derived components and derivatives [9–11]. For ethanol, the overall photoreforming reaction is expressed by Reaction (1).

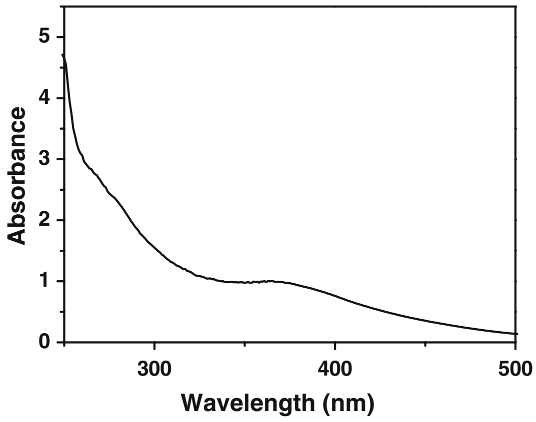

Fig. 3 Absorption spectrum of the solution obtained after 20 h PEC treatment of the 1.0 mol L^{-1} NaOH + 50%v. EtOH electrolyte

Results of the present study show that photocatalytic treatment of aqueous solutions of ethanol does not result only in oxidation of the substrate toward compounds of progressively lower molecular weight (e.g., acetaldehyde) and, eventually, CO_2 but also to the production of compounds of higher molecular weight (e.g., acetone and crotonaldehyde). The reason for this is obviously related with the setup and the experimental conditions valid with the present PEC operation. Based on results of our present and previous studies [9–11], and taking into account results of relevant investigations reported in the literature [3, 8, 20–25], a possible reaction pathway is proposed to explain the presence of the various intermediates and final products identified in the gas and liquid phase, which is summarized in Fig. 4. According to this scheme, acetaldehyde is produced by dehydrogenation of ethanol, following donation of electrons in the VB of the semiconductor [1, 8]:

$$C_2H_5OH \rightarrow CH_3CHO + H_2. \tag{2}$$

Acetaldehyde may then be photoreformed to CO_2 and H_2 (Eq. 3) or converted to acetic acid (Eq. 4), as has been proposed in the literature [1]:

$$CH_3CHO + 3H_2O \rightarrow 5H_2 + 2CO_2 \tag{3}$$

$$CH_3CHO + H_2O \rightarrow CH_3COOH + H_2. \tag{4}$$

Interestingly, acetic acid has not been detected by GC/MS in the present study. A possible explanation is that

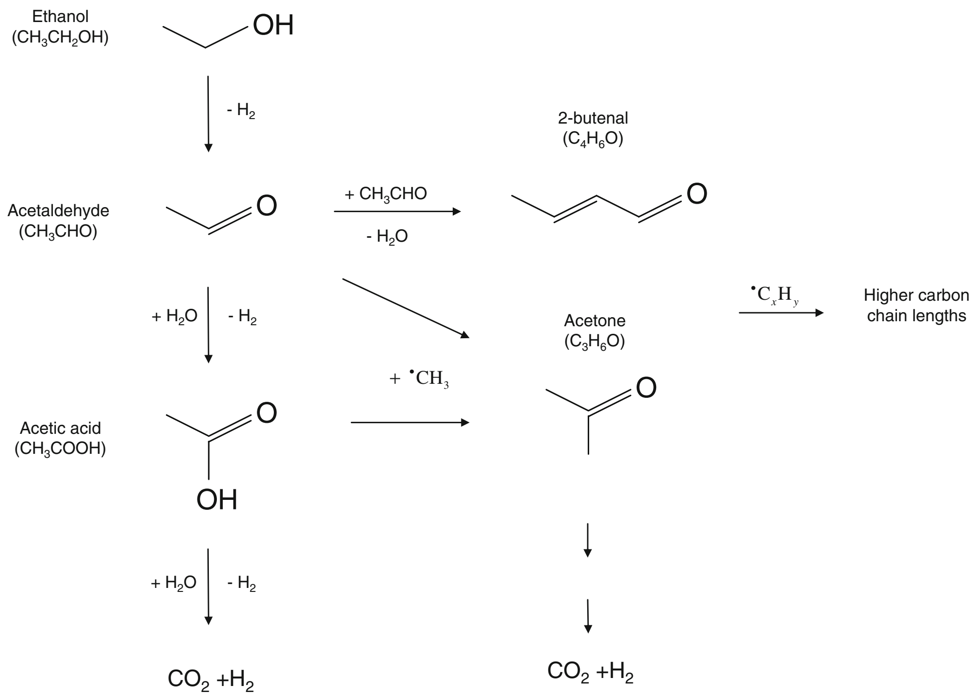

Fig. 4 Proposed reaction pathway

it was evaporated during Rotavapor condensation. It is also possible that under the present experimental conditions, i.e., in the presence of NaOH, acetic acid is present in the form of sodium acetate and hence not detected. Nevertheless, its intermediate formation should not be excluded from the reaction pathway. Sakata and Kawai [1], who investigated the present system with the use of Pt/TiO_2 photocatalyst suspensions, considered intermediate formation of acetic acid as the most probable path for the production of gas phase CH_4 and CO_2, observed in their experiments. It is well known that in the absence of oxygen and in mixed aqueous/organic solutions, aliphatic carboxylic acids are decarboxylated to the corresponding reduced hydrocarbon dimers [20]. For acetic acid, these reactions should result in the production of methane and CO_2 (Eq. 5) as well as hydrogen and ethane (Eq. 6) [21]:

$$CH_3COOH \rightarrow CH_4 + CO_2 \tag{5}$$

$$2CH_3COOH \rightarrow CH_3{-}H_3 + H_2 + 2CO_2. \tag{6}$$

Under the present conditions, we were not able to detect methane or ethane in the gas phase, which is often the case in similar studies [1, 3, 21]. This may be due to the fact that production of methane by photocatalytic decomposition of acetic acid (Eq. 5) depends strongly on solution pH [22]. In particular, it has been reported that the rate of methane evolution decreases sharply with increasing solution pH and ceases above ca. pH 8 where hydrogen evolves, almost exclusively, at the expense of methane [22]. Thus, under the present experimental conditions (solution pH 13.6) the major products formed from acetic acid should be H_2 and CO_2, according to the following Reaction (7), the validity of which has been proven in our previous study [10].

$$CH_3COOH + 2H_2O \rightarrow 2CO_2 + 4H_2 \tag{7}$$

It should be noted that Eqs. 1–7 correspond to the overall reactions that take place in the present system. Oxidation reactions occur on TiO_2 electrode and utilize the strong oxidation potential of photogenerated holes to produce oxidized species, reactive radicals and protons (e.g., Eqs. 8–11).

$$h^+ + H_2O \ \rightarrow {}^{\bullet}OH + H^+ \tag{8}$$

$$2h^+ + CH_3CH_2OH \rightarrow CH_3CHO + 2H^+ \tag{9}$$

$$2h^+ + CH_3CHO + H_2O \rightarrow CH_3COOH + 2H^+ \tag{10}$$

$$2h^+ + CH_3COO^- \rightarrow CO_2 + {}^{\bullet}\,CH_3 \tag{11}$$

Hydrogen production takes place on the Pt electrode and involves reduction of protons by photogenerated electrons according to the following equation:

$$2e^- + 2H^+ \rightarrow H_2. \tag{12}$$

Reduction of water is therefore aided by the reducing power of ethanol and reaction intermediates.

So far, discussion has been restricted to photoreforming reactions, which are known to lead, eventually, to production of H_2 and CO_2 [9–11]. However, production of compounds of higher molecular weight than that of reactant ethanol (e.g., acetone and crotonaldehyde) shows that, under the present experimental conditions, reactions relevant to organic synthesis are also operable. It is well known that several organic reactions can take place in semiconductor-mediated photocatalysis including selective oxidation, dimerization, isomerization, hydrogenation, cycloreversion, etc., [23–25]. Thus, detection of acetone, crotonaldehyde and other high molecular weight products under the present conditions is not surprising. A possible route for the production of 2-butenal (crotonaldehyde) is aldol condensation of acetaldehyde:

$$2CH_3CHO \rightarrow CH_3CH{=}CHCHO + H_2O. \qquad (13)$$

The reaction may proceed with intermediate formation of $^\bullet CH_3CHO$ radicals. Similarly, acetone can be produced by interaction of acetaldehyde (or acetic acid) with $^\bullet CH_3$ radicals.

$$CH_3CHO\ (\text{or } CH_3COOH) \xrightarrow{^\bullet CH_3} CH_3COCH_3. \qquad (14)$$

Interaction of organic radicals ($^\bullet C_xH_y$) with the various intermediates and products present on the photocatalyst surface and/or in solution may lead to the production of molecules with progressively higher carbon chain lengths and thus explain the presence of unidentified high molecular weight organic compounds detected in the present study. These high molecular weight intermediates are most probably responsible for the pale yellow color that the photooxidized solution obtained. In particular, crotonaldehyde presents a strong $\pi \rightarrow \pi^*$ absorption at about 217–227 nm and a weak $n \rightarrow \pi^*$ absorption in the UVA spectral region, strongly affected by the nature of the solvent [26]. Such behavior could justify the absorption spectrum of Fig. 3, not excluding absorption by other non-identified species.

4 Conclusion

The generally accepted scheme of photocatalytic ethanol oxidation is the step by step creation of products of progressively lower molecular weight until complete mineralization, according to the photoreforming Reaction (1), which leads solely to the production of hydrogen and carbon dioxide. This is true for the purely PC operation. However, in a PEC operation in a strongly alkaline environment in the photoanode compartment, substances of high molecular weight might be synthesized. These substances may be more resistant to photooxidation and this will make the process slower and the cell efficiency lower.

Acknowledgments We are grateful to Dr. V. Bekiari for useful discussions concerning this work. Financial support from the Program PENED (03EΔ607) of the General Secretariat of Research and Technology Hellas is graciously acknowledged.

References

1. Sakata T, Kawai T (1981) Chem Phys Lett 80:341
2. Sabate J, Cervera-March S, Simarro R, Gimenez J (1990) Int J Hydrogen Energy 15:115
3. Bamwenda GR, Tsubota S, Nakamura T, Haruta M (1995) J Photochem Photobiol A 89:177
4. Ashokkumar M (1998) Int J Hydrogen Energy 23:427
5. Galinska A, Walendziewski J (2005) Energy Fuels 19:1143
6. Blount MC, Buchholz JA, Falconer JL (2001) J Catal 197:303
7. Mizukoshi Y, Makise Y, Shuto T, Hu J, Tominaga A, Shironita S, Tanabe S (2007) Ultrason Sonochem 14:387
8. Nada AA, Barakat MH, Hamed HA, Mohamed NR, Veziroglu TN (2005) Int J Hydrogen Energy 30:687
9. Patsoura A, Kondarides DI, Verykios XE (2006) Appl Catal B 64:171
10. Patsoura A, Kondarides DI, Verykios XE (2007) Catal Today 124:94
11. Kondarides DI, Daskalaki VM, Patsoura A, Verykios XE (2008) Catal Lett 122:26
12. Strataki N, Bekiari V, Kondarides DI, Lianos P (2007) Appl Catal B 77:184
13. Strataki N, Lianos P (2008) J Adv Oxid Technol 11:111
14. Kaneko M, Nemoto J, Ueno H, Gokan N, Ohnuki K, Horikawa M, Saito R, Shibata T (2006) Electrochem Commun 8:336
15. Antoniadou M, Bouras P, Strataki N, Lianos P (2008) Int J Hydrogen Energy 33:5045
16. Bak T, Nowotny J, Rekas M, Sorrell CC (2002) Int J Hydrogen Energy 27:991
17. Nada AA, Hamed HA, Barakat MH, Mohamed NR, Veziroglu TN (2008) Int J Hydrogen Energy 33:3264
18. Mills A, Elliott N, Hill G, Durrant JR, Willis RL (2003) Photochem Photobiol Sci 2:591
19. Stylidi M, Kondarides DI, Verykios XE (2003) Appl Catal B 40:271
20. Carp O, Huisman CL, Reller A (2004) Prog Solid State Chem 32:33
21. Kraeutler B, Bard AJ (1978) J Am Chem Soc 100:5985
22. Sakata T (1989) In: Serpone M, Pelizzetti E (eds) Photocatalysis: fundamentals and applications, chapter 10: heterogeneous catalysis at liquid–solid interfaces. Wiley, New York
23. Fox MA (1983) Acc Chem Res 16:314
24. Kisch H (1994) J Prakt Chem 336:635
25. Herrmann JM, Duchamp C, Karkmaz M, Hoai BT, Lachheb H, Puzenat E, Guillard C (2007) J Hazard Mater 146:624
26. Bayliss NS, McRae EG (1954) J Phys Chem 58:1006